TECHNICAL MEMORANDUM

177

Atmospheric instability and ensemble weather prediction

F. Molteni R. Mureau and T.N. Palmer

Research Department

February 1991

European Centre for Medium-Range Weather Forecasts
Europäisches Zentrum für mittelfristige Wettervorhersage
Centre européen pour les prévisions météorologiques à moyen

Despite considerable development in numerical weather prediction techniques, substantial forecast failures still arise in situations where atmospheric evolution is particularly sensitive to the specification of initial state, ie when the intrinsic predictability of the flow is low. Predictability in the initial phase of the forecast, where error growth is linear, is studied here in terms of the largest singular value of a linearised integral evolution operator. The modes of instability associated with these singular values are used to form a set of initial states for an ensemble of predictions from a high-dimensional nonlinear weather prediction model. The dispersion of this ensemble gives an *a priori* estimate of forecast reliability beyond the range in which forecast errors have linear growth.

Consider a real N-dimensional dynamical system with state-vector X, whose evolution equation is

$$\frac{dX}{dt} = F[X] \tag{1}$$

The evolution of a small perturbation δX is determined by the linearised counterpart of (1) which can be written as

$$\frac{d\delta X}{dt} = L\delta X \tag{2}$$

where L is the Jacobian of F evaluated at some time t. Integrating over some portion of trajectory for $t_0 \le t \le t_1$, we can write (2) in integral form

$$\delta X(t_1) = A(t_1,t_0)\delta X(t_0) \tag{3}$$

Consider the matrix ΔX whose columns comprise a set of N orthogonal perturbations δX_i, $1 \le i \le N$ with amplitude ϵ. ΔX defines an error ball in phase space with covariance

$$\Delta X^*(t_0)\Delta X(t_0) = \epsilon^2 I \tag{4}$$

at t_0. Here I is the identity matrix, and '*' denotes the matrix transpose (or operator adjoint). Using (3), the error covariance at t_1 is

$$\Delta X^*(t_0)(A^*(t_1,t_0)A(t_1,t_0))\Delta X(t_0) \tag{5}$$

which defines an ellipsoid whose semi-axes have length proportional to the singular values of A, ie the square roots of the eigenvalues of the symmetric operator $A^*(t_1,t_0)A(t_1,t_0)$. For more details see Lorenz (1965) and LaCarra et al. (1988).

In conventional analysis of low-order systems, these singular values are evaluated in the limit $t_1 - t_0 \to \infty$, giving the Lyapunov exponents of 1), which characterise many of the global properties of the associated attractor. Positive Lyapunov exponents exist for low-dimensional models of large-scale atmospheric motion (eg Malguzzi et al., 1990), indicating the existence of a strange attractor for atmospheric dynamics. However, the Lyapunov exponents are not useful if one is interested in local predictability properties of the atmospheric attractor, ie the dependence of perturbation growth on initial state. In addition any perturbation consistent with realistic uncertainties in the the initial values of global atmospheric fields will become highly nonlinear before the limit $t_1 - t_0 \to \infty$ is reached.

With the analysis above, we define an index of linear instability $I_L(t_1,t_0)$ as equal to the matrix 2-norm of A , so that

$$I_L(t_1,t_0) = \|A(t_1,t_0)\| = \max_{\delta X \neq 0} \frac{\|A(t_1,t_0)\delta X(t_0)\|}{\|\delta X(t_0)\|} \qquad (6)$$

is equal to the largest singular value of A (see eg (Strang, 1980)). The inverse of $I_L(t_1,t_0)$ can be taken as a measure of linear predictability. Because A itself is not symmetric, error growth rates inferred from its singular values can be very much larger than those inferred from its eigenvalues (Farrell, 1990). Consequently predictability estimates made from normal-mode instability calculations can be erroneously optimistic.

For extratropical weather systems, the time beyond which realistic initial perturbations become nonlinear is typically a few days (see below), well before the limit of deterministic predictability (about 2 weeks) is reached. Hence, for estimating predictability beyond the first few days of integration, a linearised analysis of error growth is not appropriate. On the other hand, a rigorous treatment of error growth in the nonlinear phase would require finding an appropriate closure for equations describing the evolution of the moments of the probability density function for atmospheric error fields, a problem currently unsolved.

A possible procedure would be to integrate the full nonlinear model from an ensemble of initial states, the difference between any two members of the ensemble being consistent with uncertainties in the initial state (Leith, 1974, Hoffman et al., 1983). However, since current numerical weather prediction models comprise more than a million scalar equations, integration of an ensemble with size $M \ll N$ in which initial perturbations are chosen randomly is likely to suffer acutely from sampling problems. In particular, it is unlikely that such perturbations would have sufficient projection onto those phase-space directions which limit predictability. As a potentially viable compromise, we incorporate the linearised analysis above with the nonlinear ensemble integration procedure. Specifically, we integrate the full nonlinear model from an ensemble of states which differ from the unperturbed initial state by multiples of those eigenvectors of $\boldsymbol{A}^*\boldsymbol{A}$ which have the largest eigenvalues (cf the suggestion at the end of Lorenz, 1965).

Adapting (6), we can define an index of instability $I_{NL}(t_1,t_0)$, applicable in the nonlinear phase error growth, to be given by

$$I_{NL}(t_1,t_0)=\max_{i=1,M}\frac{\|\delta\boldsymbol{X}_i(t_1)\|}{\|\delta\boldsymbol{X}_i(t_0)\|} \tag{7}$$

where the index i spans the forecast ensemble of size M (here M=40), and where $\delta\boldsymbol{X}_i(t_1)$ is the difference in the height of the 500hPa pressure surface between perturbed integration i and the control (unperturbed) integration. Here, the norm is the rms value over the northern extratropics. By choosing the instability modes as initial perturbations, we hope to minimise the chance that the dispersion of the ensemble will underestimate the predictability of the flow, and thereby overestimate forecast reliability.

The nonlinear model used to integrate the ensemble forecasts is the European Centre for Medium-Range Weather Forecasts (ECMWF) numerical weather prediction model (Simmons et al., 1989). The basic model variables are expressed in terms of series of spherical harmonic coefficients on 19 vertical levels from the ground to the stratosphere. In the version used here, the series are truncated at total wavenumber 63 (T63). In order to investigate the full spectrum of modes, eigenvectors of the linearised operator $\boldsymbol{A}^*\boldsymbol{A}$ were calculated in a 3-level quasi-geostrophic (QG) model truncated at total wavenumber 21. In such a QG model, winds and temperatures can be derived from a single prognostic variable, potential vorticity (Gill, 1982). The modes were calculated so to maximise the growth of kinetic energy, over 1/2, 1, 2 and 4 day intervals.

Four case studies of 5-day forecasts have been made from initial dates t_0= 2 December 1988, 17 January 1989, 27 January 1989 and 1 March 1989. Among the control forecasts, the integration from 27 January was by far the poorest. In particular, the development of a large amplitude pressure ridge over the north Pacific by day 5 was substantially underestimated (see Fig.1). As a consequence, severe weather over the west coast of north America was not well forecast.

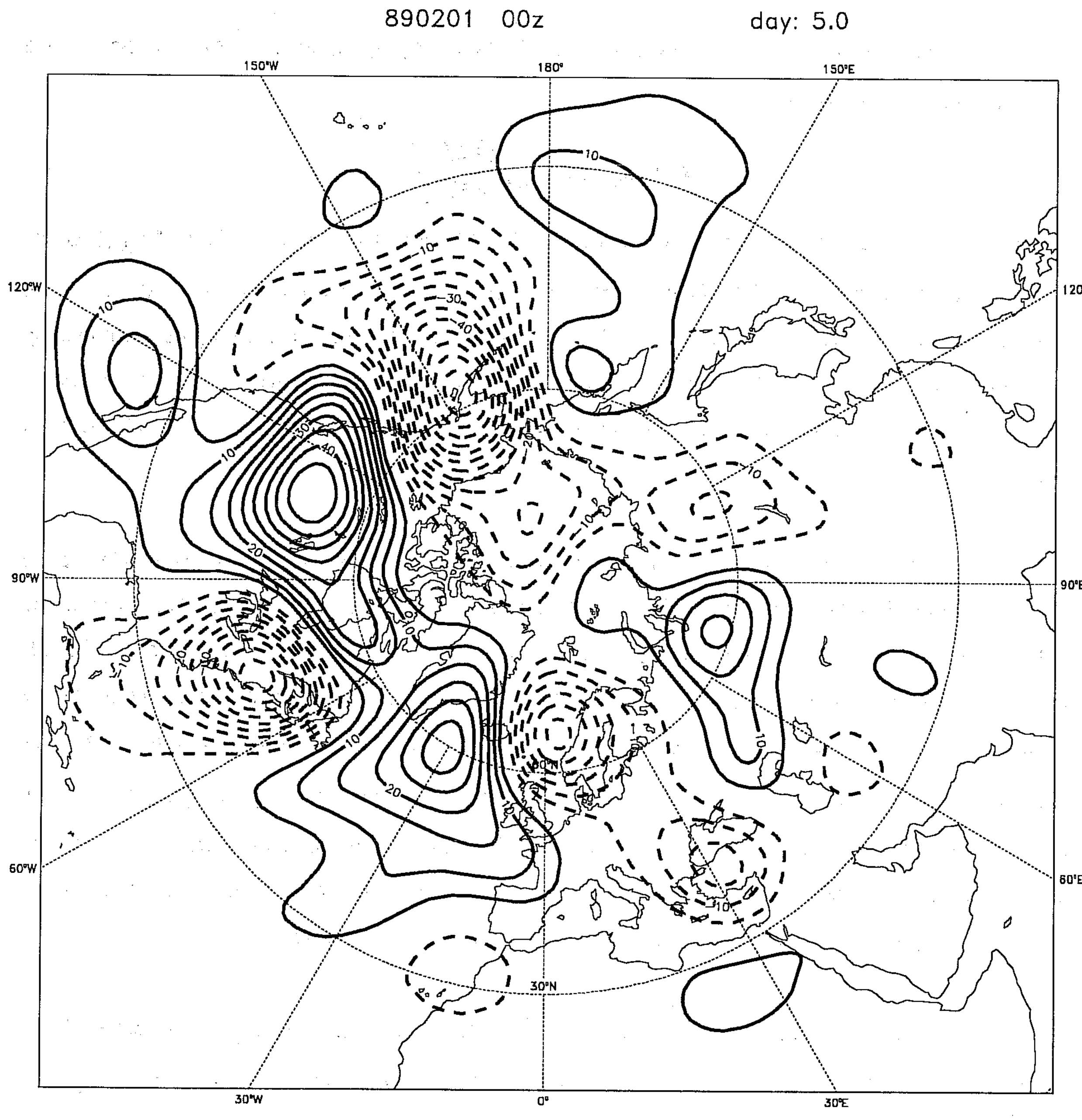

Fig.1 Day 5 forecast error of 500hPa height field of unperturbed control forecast (T63) from 00 UTC 27 January 1989. Negative values dashed. Contour interval 5 dam.

The rms errors in the prediction of the 500hPa height for the northern extratropics are given in Fig.2a for the 4 control forecasts. The linear instability index $I_L(t_0+\delta t,t_0)$ for the 4 initial dates, and for δt=1/2, 1, 2, 4 days is shown in Fig.2b. For each forecast range, the third case (from 27 January 1989) has the largest instability index, and therefore smallest predictability, though the difference becomes significant only beyond day 2. It can be seen that the variations in the values of $I_L(t_0+\delta t,t_0)$ would have given a fair a priori indication of the relative skill of the control forecasts.

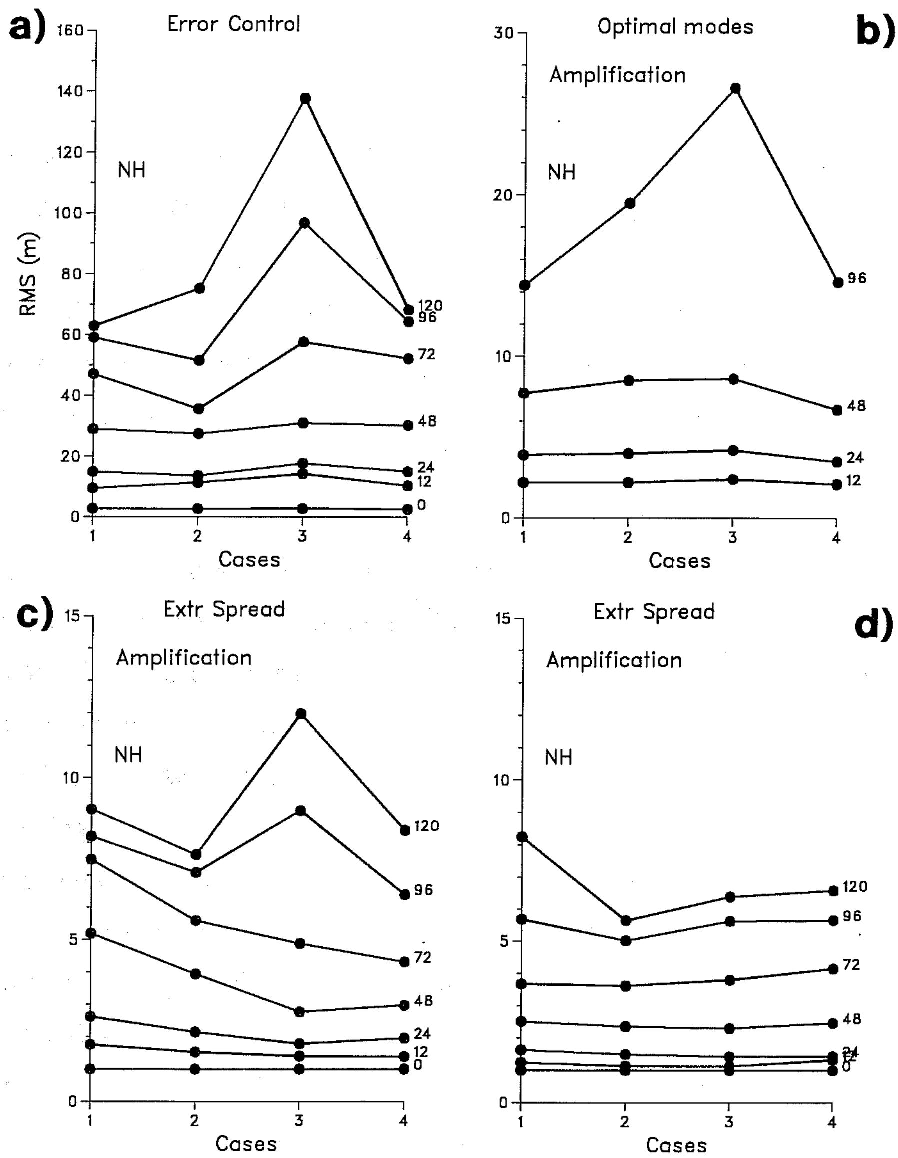

Fig.2 a) root mean square error over the northern hemisphere in the height of the 500hPa surface between four forecasts of the T63 ECMWF model. Initial dates given by 1=2 December 1988, 2=17 January 1989, 3=27 January 1989, 4=1 March 1989. b) linear instability index computed over δt=1/2, 1, 2, 4 day portions of the trajectory of the control forecast. c) nonlinear instability index calculated from the 'mode' ensemble, d) nonlinear instability index calculated from the 'non-mode' ensemble.

For each t_0, two sets of T63 ensemble forecasts were made. In the first set, the 20 fastest growing eigenvectors of $\boldsymbol{A}^*\boldsymbol{A}$, computed over 12 hour trajectories of the QG model, were interpolated onto the T63 model grid. In order to assess the results of this 'mode' ensemble against one in which the initial perturbations were not dynamically constrained, we have run a second, 'non-mode', ensemble in which the initial perturbations were based on 6 hour errors from previous archived forecasts (and are thus meteorologically balanced and representative of possible initial errors). In both sets, $\|\delta X_i(t_0)\| = 10m \quad \forall i$, and in every case, each perturbation was both added to, and subtracted from the unperturbed analysis.

The nonlinear instability estimate $I_{NL}(t_0+\delta t, t_0)$, $\delta t =$ 1/2, 1, 2, 3, 4 and 5 days for the mode and non-mode ensembles is given in Fig.2c,d for the four initial dates. For the mode ensemble, the relatively poor forecast from 27 January is picked out beyond day 4 as having the largest nonlinear instability index. By contrast, predictability estimates from the non-mode ensemble do not show any evidence of large error growth for case 3. The initial growth rates of the mode perturbations in the T63 model are consistent with the linear QG growth rates, and are substantially faster than the initial growth rates of the non-mode perturbations (see Fig.2).

The initial structure of the fastest growing linear QG mode for the 27 January case is shown in Fig.3a (in terms of the perturbation to the 500hPa surface). The amplitude of the mode is largest over the western Pacific in a region of intense atmospheric cyclogenesis. The day-5 difference between the T63 model integration initialised with this mode, and the control integration is shown in Fig.3b,c, for both positive and negative phase. It can be seen that by day 5 the disturbances have propagated downstream as far as the USA, and that the evolution of the perturbations is highly nonlinear. The perturbation shown in Fig.3b is the one with largest northern hemisphere amplitude amongst all the ensemble members, and therefore determines the nonlinear predictability index at day 5. Remarkably, the error in 500hPa height for the control forecast (Fig.1) is highly negatively correlated with the difference fields in Fig.3b, indicating that the perturbed forecast is much better that the control. For this integration, this substantial improvement is maintained when the integations are continued to day 10, well beyond the range of validity of the linear approximation to error growth.

On the basis of the results above, a forecaster would have been able to use either the linear instability index, or the nonlinear instability index from the mode ensemble (but not the non-mode ensemble) to give warning that the control forecast from the 27 January was likely to be unreliable. Moreover, using the weather elements forecast in some of the mode ensemble integrations, a warning of the possibility of severe weather over the west coast of the USA, mis-forecast in the control integration, could have been issued. On the other hand, some caution is required here, as an assessment of the statistical significance of these results will require many more cases to be studied. In practice it appears that there may be as many as 50 or more modes with energy growth rates as large as typical forecast error growth rates. On this basis it may be necessary to further select subsets of these perturbations, on the basis of their growth in the intermediate nonlinear QG model, for the construction of the initial ensemble for the T63 model. On the other hand, with projected developments in computer power, operational weather prediction with ensembles comprising some tens of forecasts may be feasible in a few years.

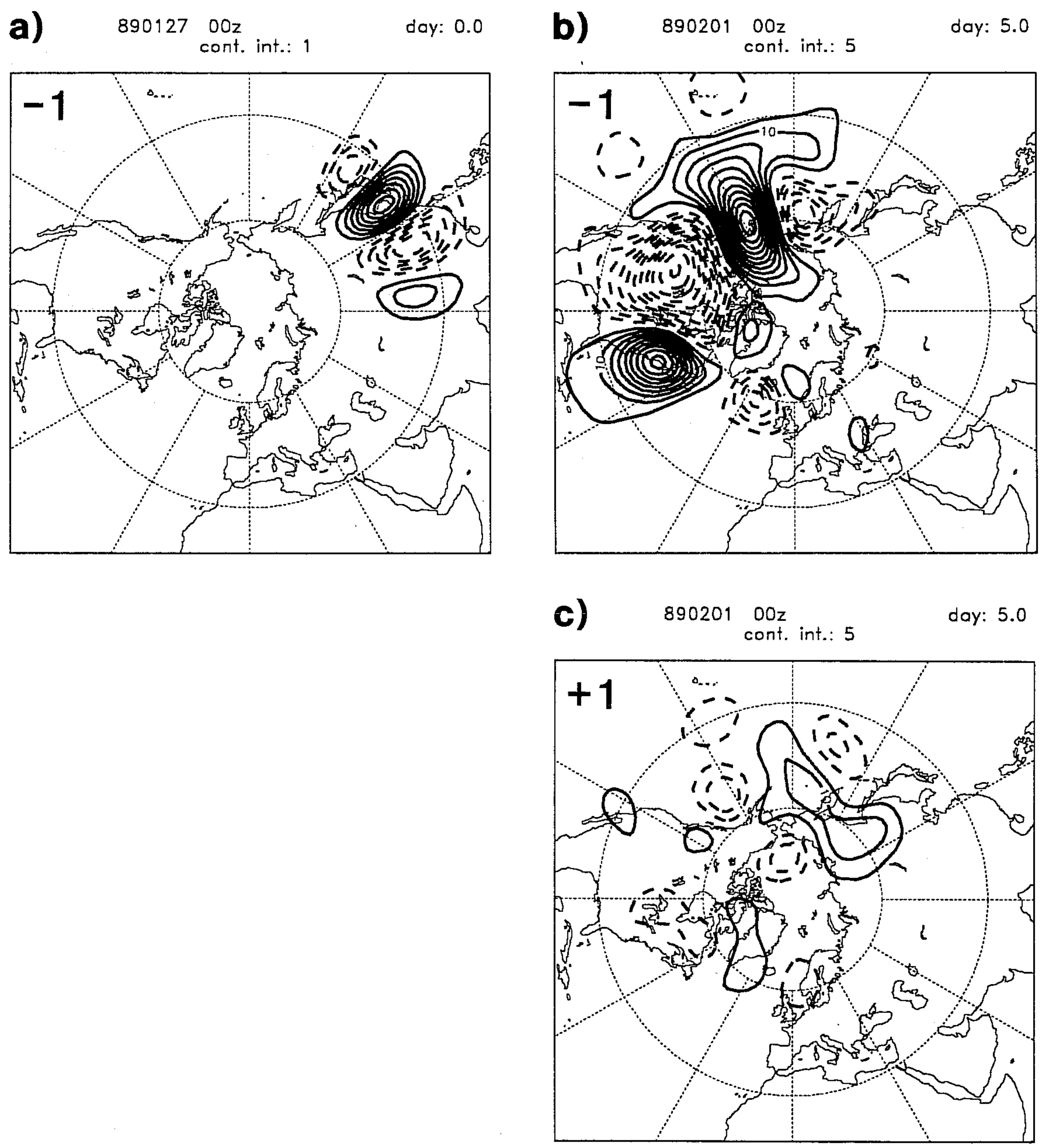

Fig.3 Development of perturbation in the ECMWF T63 model computed as having the largest eigenvalue of A^*A. Difference in 500hPa height from control forecast trajectory from 27 January case. a) day 0, b) day 5, c) day 5 from perturbation with opposite sign to that in a). Contour interval 1 dam in a), 5 dam in b) and c).

References

Farrell, B.F., 1990: Small error dynamics and the predictability of atmospheric flows. J. Atmos. Sci., 47, 2409-2416.

Gill, A.E., 1982. Atmosphere-Ocean Dynamics. International Geophysics Series, 30. Academic Press.

Hoffman R.N. and E. Kalnay, 1983. Lagged averaged forecasting. Tellus, 35a, 100-118.

LaCarra, J.-F. and O. Talagrand, 1988. Short-range evolution of small perturbations in a barotropic model. Tellus, 40A, 81-95.

Leith, C.E., 1974. Theoretical skill of Monte Carlo Forecasts. Mon.Wea.Rev., 102, 409-418.

Lorenz, E.N., 1965. A study of the predictability of a 28-variable atmospheric model. Tellus, 17, 3-33.

Malguzzi, P., A.Trevisan and A.Speranza, 1990. Statistics and predictability for an intermediate dimensionality model of the baroclinic jet. Annales Geophysicae, 8, 29-36.

Strang, G., 1980. Linear Algebra and its Applications. Academic Press. New York. 414pp.

Simmons, A.J., D.M. Burridge, M.Jarraud, C.Girard and W.Wergen, 1989. The ECMWF medium-range prediction models: Development of the numerical formulations and the impact of increased resolution. Meteor. Atmos. Phys., 40, 28-60.